World Academy of Science, Engineering and Technology
International Journal of Energy and Environmental Engineering
Vol:13, No:7, 2019

Analysis of Pressure Drop in a Concentrated Solar Collector with Direct Steam Production

Sara Sallam, Mohamed Taqi, Naoual Belouaggadia

***Abstract*—**Solar thermal power plants using parabolic trough collectors (PTC) are currently a powerful technology for generating electricity. Most of these solar power plants use thermal oils as heat transfer fluid. The latter is heated in the solar field and transfers the heat absorbed in an oil-water heat exchanger for the production of steam driving the turbines of the power plant. Currently, we are seeking to develop PTCs with direct steam generation (DSG). This process consists of circulating water under pressure in the receiver tube to generate steam directly into the solar loop. This makes it possible to reduce the investment and maintenance costs of the PTCs (the oil-water exchangers are removed) and to avoid the environmental risks associated with the use of thermal oils. The pressure drops in these systems are an important parameter to ensure their proper operation. The determination of these losses is complex because of the presence of the two phases, and most often we limit ourselves to describing them by models using empirical correlations. A comparison of these models with experimental data was performed. Our calculations focused on the evolution of the pressure of the liquid-vapor mixture along the receiver tube of a PTC-DSG for pressure values and inlet flow rates ranging respectively from 3 to 10 MPa, and from 0.4 to 0.6 kg/s. The comparison of the numerical results with experience allows us to demonstrate the validity of some models according to the pressures and the flow rates of entry in the PTC-DSG receiver tube. The analysis of these two parameters' effects on the evolution of the pressure along the receiving tub, shows that the increase of the inlet pressure and the decrease of the flow rate lead to minimal pressure losses.

***Keywords*—**Direct steam generation, parabolic trough collectors, pressure drop.

I. Introduction

LIQUID-VAPOR flows are present in many industrial applications. In the solar field, we find these flows in the new generations of solar PTCs with DSG. By convective exchanges between the water and the receiver tube, the two-phase liquid-vapor flow has several configurations along the tube. Control of this process is complex and remains a hot topic for proper PTC design. In the present work, we are interested in a numerical study of the pressure losses of a liquid-vapor flow in the absorber tube. First, we present the models describing these pressure drops. These are the approaches developed by [1]-[5]. Then, a comparison of these models with experimental data obtained on the Direct Solar Steam (DISS) Test facility installation located at the solar platform of Almería, Spain is carried out. In order to ensure a good control of the operating conditions at the entrance of the PTC receiver tube, the effect of the inlet flow and pressure is analyzed on the evolution of the pressure along the receiver tube.

S.Sallam and M. Taqi are with the Laboratory of Engineering and Materials (LIMAT), Faculty of Sciences Ben M'Sik, Hassan II University of Casablanca, Morocco (phone: +212618540787; e-mail: sallam.sara@ymail.com).

N. Belouaggadia is with the Laboratory of signals, distributed systems and artificial Intelligence, ENSET, Hassan II University, Mohammedia, Morocco.

II. Pressure Drops Models

The total two-phase pressure drop (ΔP_{tp}) in a boiling system consists of three components: the acceleration pressure drop (ΔP_{acc}), gravitational pressure drop (ΔP_{grav}) and frictional pressure drop (ΔP_{fr}). The total pressure drop is then given by:

$$\Delta P_{tp} = \Delta P_{grav} + \Delta P_{acc} + \Delta P_{fr} \quad (1)$$

The gravitational pressure drop is null in a horizontal flow. So:

$$\Delta P_{tp} = \Delta P_{acc} + \Delta P_{fr} \quad (2)$$

The pressure drop due to the acceleration of the fluid is estimated from the model of the separate flows as presented in [6]. It is expressed as follows:

$$\Delta P_{acc} = G^2 \left\{ \left[\frac{(1-x)^2}{\rho_l(1-\varepsilon)} + \frac{x^2}{\rho_g \varepsilon} \right]_{out} - \left[\frac{(1-x)^2}{\rho_l(1-\varepsilon)} + \frac{x^2}{\rho_g \varepsilon} \right]_{in} \right\} \quad (3)$$

where ρ_l and ρ_g are respectively the density of liquid and gas, G is the total mass velocity and x is the quality of the vapor.

The void fraction ε is evaluated by semi-empirical correlations. Several works [7]-[10] recommend the use of the Steiner correlation [11] which is expressed by:

$$\varepsilon = \frac{x}{\rho_g} \left[\left(1 + 0.12\,(1-x)\right) \left(\frac{x}{\rho_g} + \frac{(1-x)}{\rho_l} \right) + \frac{1.18(1-x)[g\sigma(\rho_l - \rho_g)]^{0.25}}{G^2 \rho_l^{0.5}} \right]^{-1} \quad (4)$$

with σ is the surface tension and g is the gravity acceleration.

The pressure drop due to the friction at the wall is the most important. It is predicted by empirical approaches, the most cited being those developed by [1]-[5] which are presented in Table I.

III. Comparison of Models

To evaluate the pressure drops, we adopt the steam quality distributions obtained numerically by [12] (Fig. 1). The geometry and operating conditions are given in Table II.

TABLE I
MODELS OF PRESSURE DROPS DUE TO FRICTION

Authors	Models	Detailed
Lockhart and Martinelli [1]	$\Delta P_{frott} = \Phi^2 \Delta P_{monoph} = \Phi_l^2 \Delta P_l = \Phi_g^2 \Delta P_g$ (5)	$X = \sqrt{\frac{(dP/dz)_l}{(dP/dz)_v}} = \left(\frac{1-x}{x}\right)^{0.9} \left(\frac{\rho_v}{\rho_l}\right)^{0.5} \left(\frac{\mu_l}{\mu_v}\right)^{0.1}$ (10)
	$\Phi_l^2 = 1 + \frac{C}{X} + \frac{1}{X^2}$ (6)	C=20
	$\Phi_g^2 = 1 + CX + X^2$ (7)	The friction factors of liquid f_l and vapor f_g are calculated using the Blasius formula:
	$\Delta P_l = 4\, f_l \left(\frac{L}{D}\right) G^2 (1-x)^2 \left(\frac{1}{2\rho_l}\right)$ (8)	$f_l = \frac{0.079}{Re_l^{0.25}}$ with $Re_l = \frac{G(1-x)D}{\mu_l}$ (11)
	$\Delta P_g = 4\, f_g \left(\frac{L}{D}\right) G^2 x^2 \left(\frac{1}{2\rho_g}\right)$ (9)	$f_g = \frac{0.079}{Re_g^{0.25}}$ with $Re_g = \frac{GxD}{\mu_g}$ (12)
Grönnerud [2]	$\Delta P_{frott} = \Phi_{gd} \Delta P_{lo}$ (13)	The pressure gradient defined by Grönnerud:
	$\Phi_{gd} = 1 + \left(\frac{dP}{dz}\right)_{gd} \left[\frac{\left(\frac{\rho_l}{\rho_g}\right)}{\left(\frac{\mu_l}{\mu_v}\right)^{0.25}} - 1\right]$ (14)	$\left(\frac{dP}{dz}\right)_{gd} = f_{gd}\left[x + 4\left(x^{1.8} - x^{10} {f_{gd}}^{0.5}\right)\right]$ (17)
	Pressure losses due to friction for liquid alone (ΔP_{lo}) and vapor alone (ΔP_{go}) are calculated according to the Darcy-Weisbach relation as follows:	The coefficient f_{gd} depends on Froude number:
	$\Delta P_{lo} = 4\, f_{lo} \left(\frac{L}{D}\right) G^2 \left(\frac{1}{2\rho_l}\right)$ (15)	$\begin{cases} f_{gd} = 1 & Si \quad Fr_l \geq 1 \\ f_{gd} = Fr_l^{0.3} + 0.0055\left(ln\left(\frac{1}{Fr_l}\right)\right)^2 & Si \;\; Fr_l < 1 \end{cases}$ (18)
	$\Delta P_{go} = 4\, f_{go} \left(\frac{L}{D}\right) G^2 \left(\frac{1}{2\rho_g}\right)$ (16)	$Fr_l = \frac{G^2}{gD{\rho_l}^2}$ (19)
		The friction factors of liquid alone (f_{lo}) and vapor alone (f_{go}) are calculated using the Blasius relation:
		$f_{lo} = \frac{0.079}{Re_{lo}^{0.25}}$ with $Re_{lo} = \frac{GD}{\mu_l}$ (20)
		$f_{go} = \frac{0.079}{Re_{go}^{0.25}}$ with $Re_{go} = \frac{GD}{\mu_g}$ (21)
Chisholm [3]	$\Delta P_{frott} = \Phi_{ch}^2 \Delta P_{lo}$ (22)	For $Y \leq 9.5$
	$\Phi_{ch}^2 = 1 + (Y^2 - 1)\left[\left(B_{ch} x(1-x)\right)^{(2-n)/2} + x^{2-n}\right]$ (23)	$B_{ch} = \frac{55}{G^{1/2}} \;\; for\; G \geq 1900\, kg/m^2 s$ (25)
	n is the exponent of the expression of the friction factor of Blasius (n = 0,25). The Y^2 parameter is expressed as follows:	$B_{ch} = \frac{2400}{G} \; pour \;\; 500 < G < 1900\, kg/m^2 s$ (26)
	$Y^2 = \frac{\left(\frac{dP}{dz}\right)_{go}}{\left(\frac{dP}{dz}\right)_{lo}}$ (24)	$B_{ch} = 4.8 \quad for\; G \leq 500\, kg/m^2 s$ (27)
		For $9.5 < Y < 28$
		$B_{ch} = \frac{520}{YG^{1/2}} \;\; for\; G \leq 600\, kg/m^2 s$ (28)
		$B_{ch} = \frac{21}{Y} \;\; for\; G > 600\, kg/m^2 s$ (29)
	ΔP_{lo} is evaluated by (15) and (20).	For $Y \geq 28$
		$B_{ch} = \frac{15000}{Y^2 G^{1/2}}$ (30)
Friedel [4]	$\Delta P_{frott} = \Phi_{fr}^2 \Delta P_{lo}$ (31)	The number of homogeneous Froude ((Fr_h)), the number of Weber (We), the coefficients E, F and H are the following:
	$\Phi_{fr}^2 = E + \frac{3.24\, FH}{Fr_h^{0.045} We_l^{0.035}}$ (32)	$Fr_h = \frac{G^2}{gD\rho_h^2}$ (33)
	ΔP_{lo} is evaluated by (15) and (20).	$E = (1-x)^2 + x^2 \frac{\rho_l f_{go}}{\rho_g f_{lo}}$ (34)
		$F = x^{0.78}(1-x)^{0.224}$ (35)
		$H = \left(\frac{\rho_l}{\rho_g}\right)^{0.91} \left(\frac{\mu_g}{\mu_l}\right)^{0.19} \left(1 - \frac{\mu_g}{\mu_l}\right)^{0.7}$ (36)
		$We = \frac{G^2 D}{\sigma \rho_h}$ (37)
		$\rho_h = \left(\frac{x}{\rho_g} + \frac{1-x}{\rho_l}\right)^{-1}$ (38)

Authors	Models		Detailed	
Müller-Steinhagen and Heck [5]	$\left(\frac{dP}{dz}\right)_{frott} = F_{msh}\,(1-x)^{1/3} + B_{msh}x^3$	(39)	$A_{msh} = \left(\frac{dP}{dz}\right)_{lo} = f_{lo}\frac{2\,G^2}{D\rho_l}$	(41)
	$F_{msh} = A_{msh} + 2\,(B_{msh} - A_{msh})x$	(40)	$B_{msh} = \left(\frac{dP}{dz}\right)_{go} = f_{go}\frac{2\,G^2}{D\rho_g}$	(42)

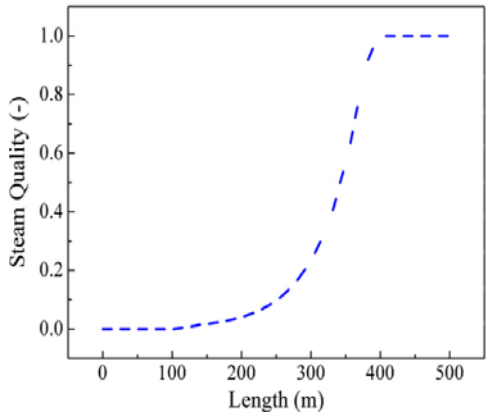

(a) Case 1

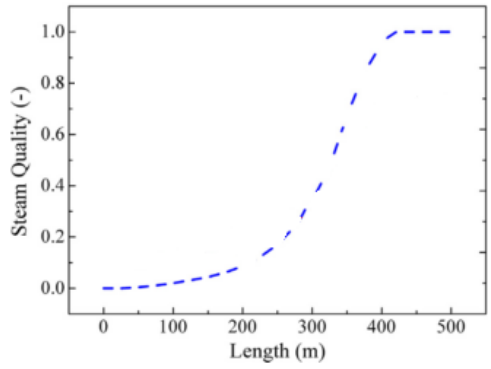

(b) Case 2

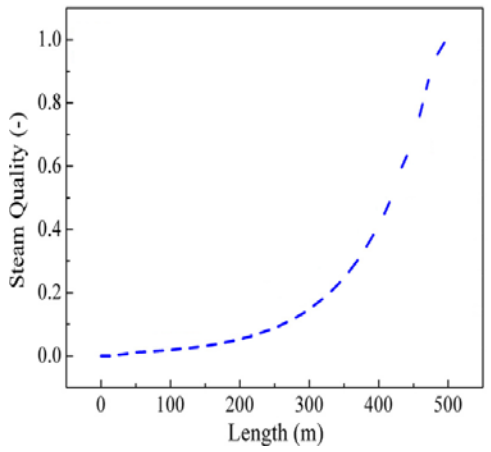

(c) Case 3

Fig. 1 Distributions of the steam quality obtained by David et al. [12]

Fig. 2 illustrates the evolution of the pressure of the liquid-vapor mixture along the receiver tube of a CCP-PDV, as a function of the steam quality, for the various models described above.

TABLE II
GEOMETRIC AND OPTICAL PROPERTIES AND THE CCP OPERATING CONDITIONS STUDIED

	Parameters	values		
Geometric properties	Absorber pipe internal diameter (m)	0.05		
	Absorber pipe external diameter (m)	0.07		
	Aperture (m)	5.76		
Optical properties	Reflected surface reflectivity	0.93		
	Glass cover transmittance	0.95		
	Receiver absorptance	0.906		
	Shape facteur	0.92		
	Inclination angle	0.0		
	Modifed incident angle	1.0		
		Case1	Case2	Case3
Operating conditions	Inlet pressure (MPa)	10.20	6.23	3.38
	Inlet temperature $(°C)$	245	235	196
	Inlet flow rate (kg/s)	0.62	0.50	0.47
	Direct Solar flux (w/m^2)	967	850	807

The different models represent the same usual trend, which results in a decrease of the pressure when the length of the pipe increases and consequently when the quality increases. The maximum difference between these models is 0.3%, 0.6% and 3.1% respectively for cases 1, 2 and 3. The comparison of these models with experimental data [12] shows that the Friedel model [4] is the closest to the experiment for cases 1 and 2 (inlet pressure and flow rate of $10.20 MPa$ and $0.62\ Kg/s$; $6.23\ MPa$ and $0.50\ Kg/s$) while the Chisholm model [3] gives the best prediction of the pressure drop for the third case (pressure and inlet flow of $3.38 MPa$ and $0.47\ kg/s$).

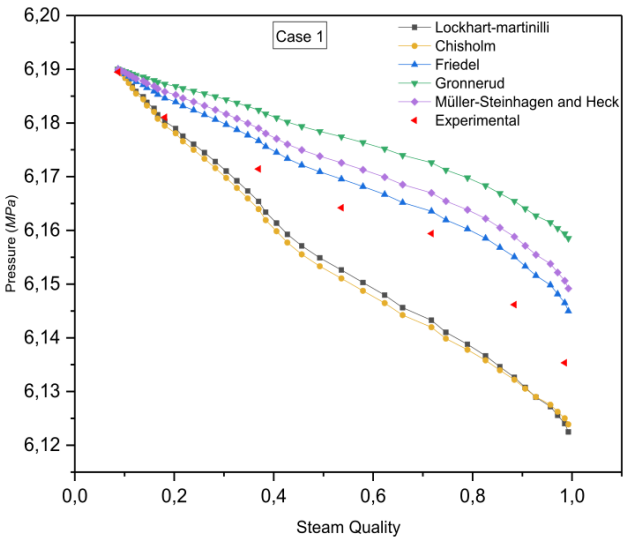

(a)

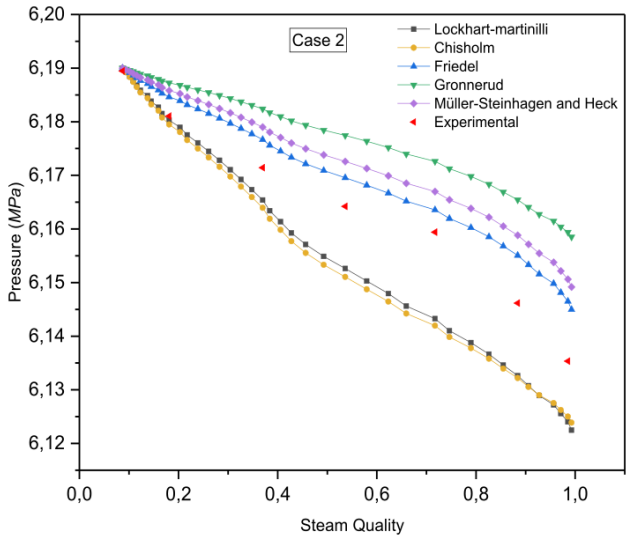

(b)

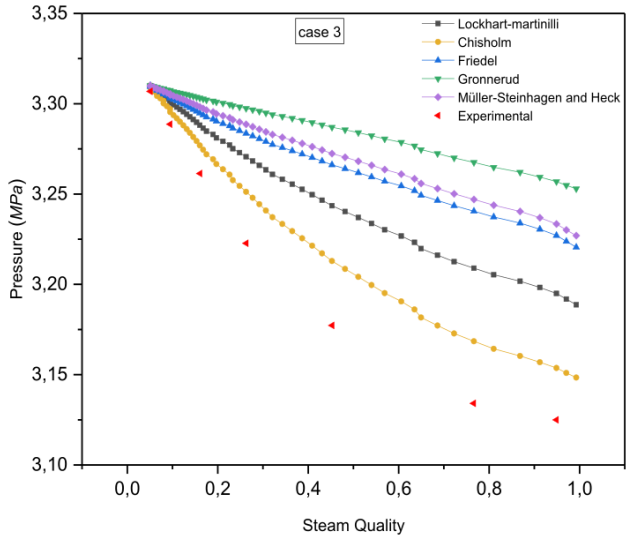

(c)

Fig.2 The evolution of the pressure as a function of the steam quality for different models for the three cases studied

According to our study, the Friedel model [4] is the most suitable for the prediction of friction losses for most of the studied operating conditions, which is also recommended by other studies [13]–[15].

IV. Analysis of Pressure Evolution

According to the comparison of the pressure drop models, the Friedel model is adopted, in order to analyze the effects of the inlet pressure and flow rate on the pressure evolution along the PTC-DSG receiving tube.

A. Input Flow Rate Effect

In order to take the effect of the input mass flow rate on the pressure evolution in the CCP-PDV receiver tube, we vary the mass flow (0.4, 0.5, $0.6kg/s$) with an inlet pressure of $6.19MPa$.

Fig. 3 illustrates the pressure evolution in the PTC-DSG receiver tube as a function of steam quality for different input flow rate. We notice that for the low quality, the input mass flow does not have a great effect. However, this effect becomes important when the quality increases. The increase in inlet flow rate increases the pressure drops, and consequently, the pressure decreases.

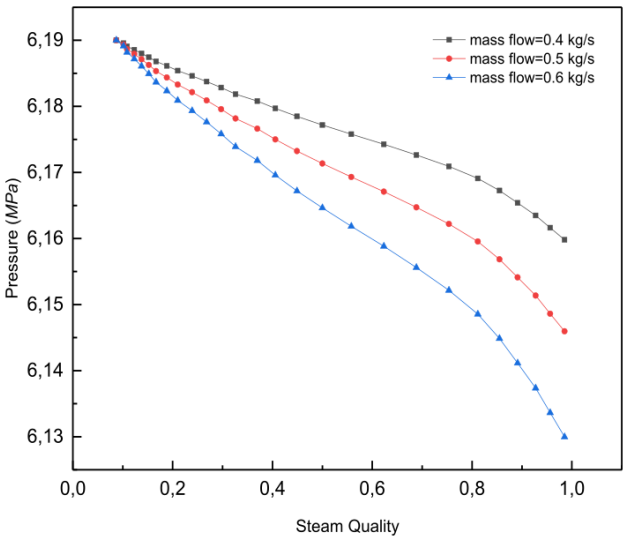

Fig. 3 Effect of input mass flow on the evolution of the pressure in the PTC-DSG receiver tube

B. Effect of Inlet Pressure

In order to analyze also the effect of the inlet pressure on the evolution of the pressure along the PTC-DSG receiver tube, the inlet pressure is varied from 3MPa to 10MPa for a flow rate of 0.6kg/s. The pressure losses in the PTC-DSG receiver tube as a function of steam quality for the different inlet pressure values are plotted in Fig. 4 (b). The pressure drops increase by increasing the steam quality. This increase becomes important when the inlet pressure decreases. So the increase in the inlet pressure ensures minimal pressure drops.

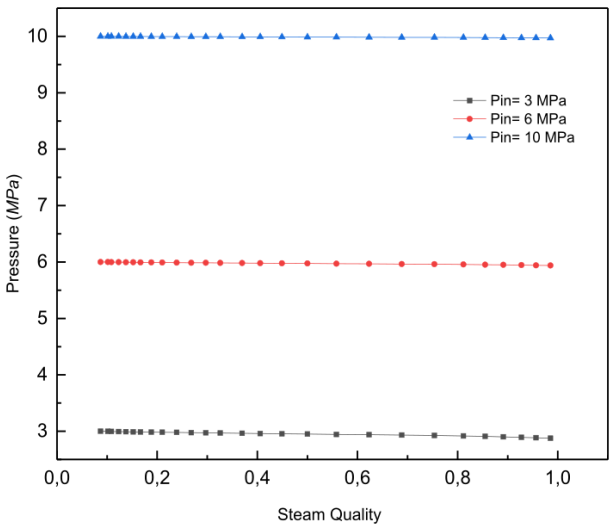

(a)

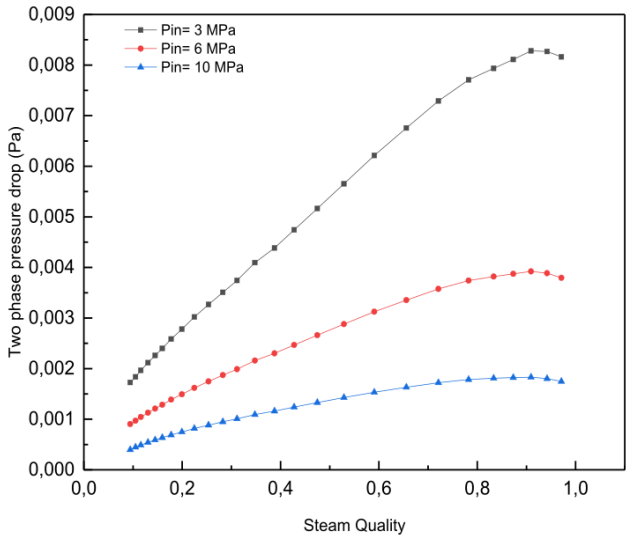

(b)

Fig. 4 Effect of inlet pressure on the evolution of pressure (a) and pressure drop (b) in the PTC-DSG receiver tube

V. Conclusion

In this work, different models describing the pressure drops in a liquid-vapor flow are presented. The calculations concern the evolution of the pressure of the liquid-vapor mixture along the receiver tube of a PTC-DSG. The pressure decreases by increasing the steam quality for all models with a small gap between them. Comparison of these models with the experimental data shows that the Friedel model [4] is closest to the experiment for high inlet pressures and flow rates whereas the Chisholm model [3] gives the best prediction of the pressure drop for a low inlet pressure and flow rate. The analysis of the effects of inlet pressure and flow rate on the evolution of the pressure along the PTC-DSG receiving tube shows that the increase of the inlet pressure and the decrease of the inlet flow rate ensure losses minimum charge.

References

[1] R. W. Lockhart and R. C. Martinelli, "Proposed correlation of data for isothermal two-phase, two-component in pipes," *Chem. Eng. Process*, vol. 45(1), pp. 39–48, 1949.

[2] R. Gronnerud, "Investigation of liquid hold-up, flow resistance and heat transfer in circulation type evaporators. 4. Two-phase flow resistance in boiling refrigerants," *Annex. 1972-1, Bull. l'Inst. du Froid*, pp. 127–138, 1972.

[3] D. Chisholm, "Pressure gradients due to friction during the flow of evaporating two-phase mixtures in smooth tubes and channels.," *Int. J. Heat Mass Transf.*, vol. 16, no. 29, pp. 347–358, 1973.

[4] L. Friedel, "Improved friction pressure drop correlations for horizontal and vertical two-phase pipe flow," *Eur. Two-phase Flow Gr. Meet. Ispra, Italy*, vol. 18, no. 2, pp. 485–492, 1979.

[5] H. Muller steinhagen and K. HECK, "A Simple Friction Pressure Drop Correlation for Two-Phase Flow in Pipes," vol. 20, no. 1, pp. 297–308, 1986.

[6] B. K. Hardik and S. V Prabhu, "International Journal of Thermal Sciences Boiling pressure drop and local heat transfer distribution of water in horizontal straight tubes at low pressure," *Int. J. Therm. Sci.*, vol. 110, pp. 65–82, 2016.

[7] M. B. O. Didi, N. Kattan, and J. R. Thome, "Prediction of two-phase pressure gradients of refrigerants in horizontal tubes´ vision des gradients de pression des frigorige ` nes en Pre ´ coulement diphasique dans des tubes horizontaux e," *Int. J. Refrig.*, vol. 25, pp. 935–947, 2002.

[8] L. Wojtan, T. Ursenbacher, and J. R. Thome, "Investigation of flow boiling in horizontal tubes : Part I — A new diabatic two-phase flow pattern map," vol. 48, pp. 2955–2969, 2005.

[9] J. M. Quibén, L. Cheng, R. J. da S. Lima, and J. R. Thome, "International Journal of Heat and Mass Transfer Flow boiling in horizontal flattened tubes : Part I – Two-phase frictional pressure drop results and model," *Int. J. Heat Mass Transf.*, vol. 52, no. 15–16, pp. 3634–3644, 2009.

[10] Z. Yang, M. Gong, G. Chen, X. Zou, and J. Shen, "Two-phase flow patterns, heat transfer and pressure drop," *Appl. Therm. Eng.*, 2017.

[11] D. Steiner, *VDI-Wärmeatlas (VDI Heat Atlas), Verein Deutscher Ingenieure, VDI-Gesellschaft Verfahrenstechnik und Chemieingenieurwesen (GCV), Düsseldorf*. 1993.

[12] H. Lobón David, B. Emilio, V. Loreto, and Z. Eduardo, "Modeling direct steam generation in solar collectors with multiphase CFD," vol. 113, pp. 1338–1348, 2014.

[13] M. Biencinto, L. González, and L. Valenzuela, "A quasi-dynamic simulation model for direct steam generation in parabolic troughs using TRNSYS," *Appl. Energy*, vol. 161, pp. 133–142, 2016.

[14] M. Eck and W.-D. Steinmann, "ISEC2004-65040 Modeling and Design of Direct Solar Steam Generating Collector Fields," *ASME*, pp. 1–10, 2004.

[15] A. Amine, I. Rodríguez, and C. Ghenai, "Thermo-hydraulic analysis and numerical simulation of a parabolic trough solar collector for direct steam generation," *Appl. Energy*, vol. 214, no. January, pp. 152–165, 2018.